Chemical Science

Accepted Manuscript

This article can be cited before page numbers have been issued, to do this please use: A. Potluri, J. B. Siegel and D. J. Tantillo, *Chem. Sci.*, 2026, DOI: 10.1039/D6SC03024F.

ROYAL SOCIETY OF CHEMISTRY

rsc.li/chemical-science

View Article Online
DOI: 10.1039/D6SC03024F

Reinvestigation of the Mechanism and Selectivity of 1,8-Cineole Synthase using *TerDockin*

Abhay Potluri, Justin B. Siegel, Dean J. Tantillo*

Department of Chemistry, University of California, Davis, 1 Shields Ave, Davis, CA 95616, USA

djtantillo@ucdavis.edu

Abstract

The mechanism of 1,8-cineole formation in *Streptomyces clavuligerus* 1,8-cineole synthase was reinvestigated using the *TerDockin* modeling approach and compared to that in *Salvia fruticosa*. The results of these simulations provided new data on the binding modes of carbocations, the nature of active site bases, and enantioselectivity. In particular, the likelihood of pathways involving *R* and *S* terpinyl cation was assessed, and differentiation of these was found to relate to the position of active site bases rather than selective binding of the carbocations.

Introduction

Terpenes and terpenoids (functionalized terpenes) are omnipresent in the natural world, constituting the largest class of natural products.[1,2] These compounds are regarded for both their skeletal and stereochemical diversity.[3] In plants, they act as predator repellents,[4] growth regulators,[5] and mediators of inter/intra-species

View Article Online
DOI: 10.1039/D6SC03024F

communication.[6] For humans, these secondary metabolites have found applications including medicines,[7–9] cosmetics,[10–12] flavor additives,[13] bio-fuels,[14] and insecticides.[15]

The enzymes that construct terpenes – terpene synthases (also called cyclases when cyclic terpenes are produced) – are split into two classes. Class I enzymes utilize a trinuclear Mg^{2+} cluster to facilitate loss of diphosphate (PP_i) from their substrates to generate a reactive allylic carbocation that initiates a cascade of hydride and/or alkyl shifts, proton transfers, and cyclizations, eventually leading to a terpene product.[16] In general, the active sites of Class I terpene synthases contain DDXXD and NSE/DTE sequence motifs that are involved in binding the Mg^{2+} ions and the diphosphate portion of the terpene precursor.[17] The remainder of the active site is composed primarily of aromatic and aliphatic amino acids that provide a shape that biases the conformations of the rearranging carbocation, while shielding it from premature quenching by basic species.[17] Class II terpene synthases also contain nonpolar carbocation binding regions but differ in the mechanism by which they trigger the formation of the carbocation. Class II enzymes utilize acidic amino acids (Asp or Glu) to protonate a π-bond or epoxide to generate a reactive carbocation.[17,18] We focus here on an unusual Class I enzyme.

Termination of the carbocation cascade in Class I enzymes is usually accomplished by PP_i in one of two ways: deprotonation or direction addition, the latter being far less common.[19–24] Occasionally, water molecules in the active site can play similar roles, sometimes adding to produce an alcohol functional group.[25–31] There are some cases, however, where water addition does not terminate the reaction but leads to an ether via subsequent addition to a nearby alkene (e.g., Figure 1).[32–35] We have examined one of these cases, formation of 1,8-cineole, using our specialized terpene synthase modeling

View Article Online
DOI: 10.1039/D6SC03024F

approach called *TerDockin*[20,36] – both to provide a new perspective on the mechanism and selectivity of this reaction and to test the performance of *TerDockin* in this nonstandard scenario.

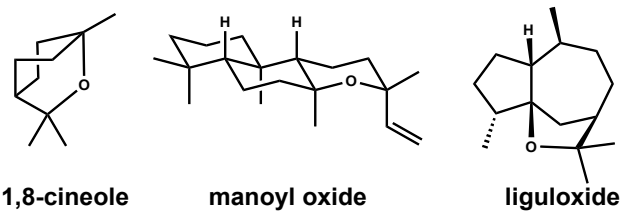

Figure 1. Examples of naturally occurring heterocyclic terpenes formed via water addition.

Scheme 1 shows a possible mechanism for the formation of 1,8-cineole.[37] This mechanistic model evolved over time. In 1977, 1,8-cineole was extracted from *Salvia officinalis* and the mechanism for its formation was proposed to utilize a cystine amino acid to activate the cyclization of neryl diphosphate.[38] In 1994, ^{2}H and ^{18}O labelling of water showed that the final product contains one ^{2}H and the ^{18}O atom.[39] Additionally, the substrate was found to be geranyl diphosphate rather than neryl diphosphate, meaning that a *trans*-*cis* isomerization occurred.[39] In 2002, a deuterated water (D_2O) experiment showed that the final product contained a deuterium, consistent with an intramolecular proton transfer during formation of the second oxonium ion intermediate (Scheme 1, **B** → **C**).[34] Additionally, it was proposed that the *gem*-dimethyl-containing group had to rotate in the active site to orient the initial oxonium ion toward the face of the alkene π-bond (Scheme 1, **A** → **B**).[34] In 2017, an X-ray crystal structure of a *Streptomyces clavuligerus*

View Article Online
DOI: 10.1039/D6SC03024F

1,8-cineole synthase revealed a water molecule in the active site close to the fluorinated geranyl diphosphate substrate analog, supporting the notion that water is the oxygen atom provider.[37] In 2020, a combination of density functional theory (DFT) calculations, molecular dynamics (MD) simulations, and mutagenesis experiments was performed on a *Streptomyces clavuligerus* 1,8-cineole synthase.[40] Mutagenesis of Asn305 to any of a variety of amino acids reduced or prevented 1,8-cineole formation. The accompanying calculations assumed Asn305 to be the catalytic base that deprotonates the oxonium ion and did not account for σ-bond rotation. We revisit these assumptions.

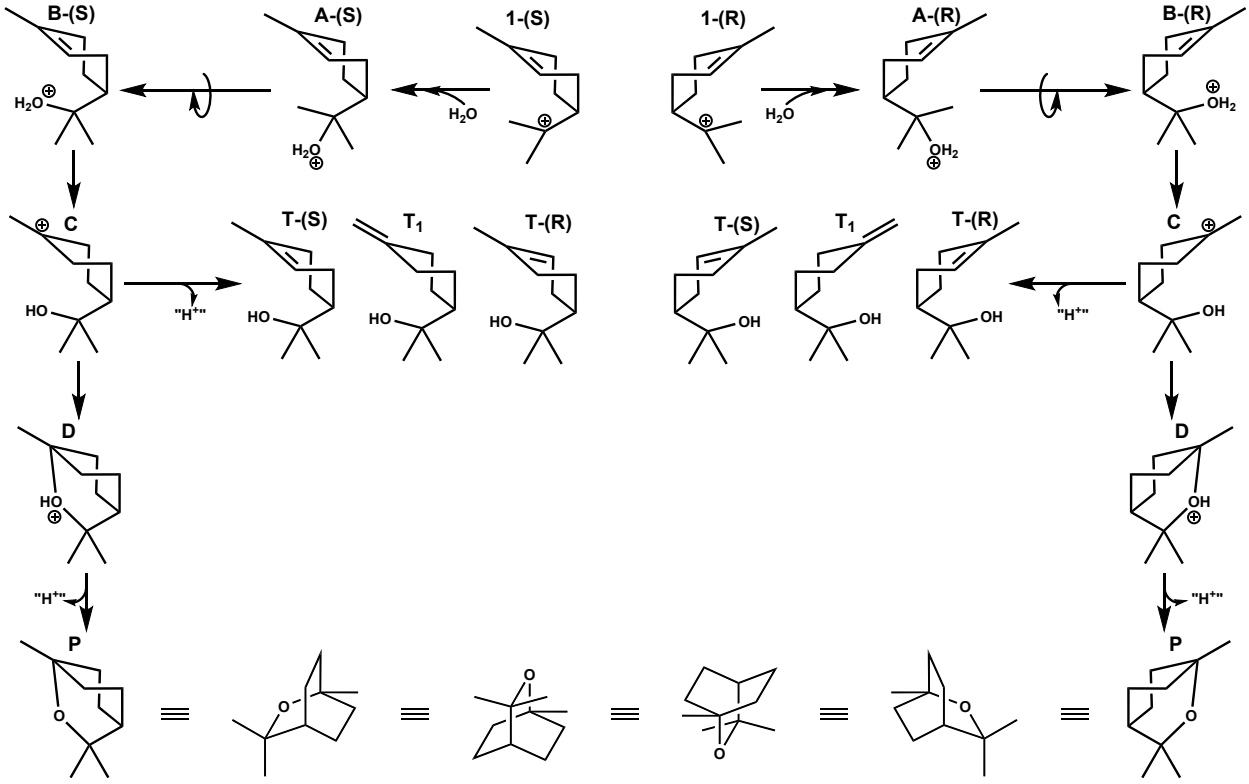

Scheme 1. Mechanism of 1,8-cineole from terpinyl cation. The minor side product, terpineol, is shown from intermediate **C**.

View Article Online
DOI: 10.1039/D6SC03024F

Here, we reexamine the mechanism of 1,8-cineole formation from the terpinyl cation, both through quantum mechanical (QM) computations on inherent reactivity[41] and computations on carbocation binding using the *TerDockin* approach[20,36] on the 1,8-cineole synthase from *Streptomyces clavuligerus* expressed in *Escherichia coli*. First, we aim to assess whether the most recently proposed mechanism (Scheme 1) is energetically viable. Similar schemes were published by Wise et al.[34] and Karuppiah et al.[37] Second, we aim to identify the most likely active site base and determine why it does not deprotonate carbocations prematurely. 1,8-Cineole synthases from *Streptomyces lividans* and *Streptomyces clavuligerus* reported low side product formation. In contrast, plant synthases from *Salvia fruticosa*, *Citrus unshiu*, *Arabidopsis thaliana*, and *Nicotiana suaveolens* form α-terpineol, β-myrcene, sabinene, and other monoterpenes.[25,42–45] Third, we use this study to assess the viability of the *TerDockin* approach, which is far less computationally demanding than molecular dynamics (MD),[46,47] to model terpene synthase reactions involving water addition. Fourth, we assess the likelihood that 1,8-cineole synthases selectively bind enantiomers of the chiral carbocations that must be generated during formation of their achiral product (Scheme 1).[20] Chiral GC analysis of the side product α-terpineol revealed that 1,8-cineole synthases from *Salvia fruticosa* accumulate more (*R*)-**T**, whereas the *Streptomyces clavuligerus* counterpart accumulates more (*S*)-**T**.[40,48] In varying *Nicotiana* species, a preference for (*S*)-**T** was observed with GC-MS.[25] These results suggest that different 1,8-cineole synthases may well prefer different carbocation enantiomers. A strong preference in any given case is also not guaranteed. For *Streptomyces clavuligerus,*

View Article Online
DOI: 10.1039/D6SC03024F

carbocation (*R*)-**1** was proposed to be the source of 1,8-cineole based on the shape of the active site in the crystal structure, but deuterium labeling experiments indicated that (*S*)-**1** is the primary reactive intermediate.[37,49] The results of the deuterium labeling experiments for *Streptomyces clavuligerus* are compelling, and we seek here to understand them in light of our models.

Methods

QM calculations were performed using *Gaussian16*.[50] DFT was used to optimize the structures of intermediates and transition structures. Initial calculations were performed using B3LYP as the functional.[51,52] B3LYP is a commonly used hybrid functional that provides reasonable geometries.[52,53] Subsequently, the functional was switched to mPW1PW91, which provides more accurate energies (in particular, for cyclization reactions).[54]

The traditionally used 6-31+G(d,p) basis set was first used, then diffuse functions were removed to speed up calculations and test whether geometries and electronic energies would still be reliable.[55] Triple-ζ basis sets were also examined. Energies reported in the main text are from mPW1PW91/6-311G(d,p) calculations; see the SI for comparisons to results from other levels. The gas phase, a crude but reasonable approximation of the nonpolar carbocation binding region of a terpene synthase active site,[53] was used throughout. Thermal corrections to energies were obtained using Paton's and Funes-Ardoiz's *GoodVibes* program, which employs the roto-harmonic

View Article Online
DOI: 10.1039/D6SC03024F

approximation.[56] Natural Bond Orbital (NBO) analysis was performed on intermediates to quantify magnitudes of orbital interactions between functional groups.[57,58,59]

Molecular docking was performed using the *Rosetta* software suite after preparation of the protein and ligands.[60–62] A crystal structure of 1,8-cineole synthase from *Streptomyces clavuligerus* (5NX7) was obtained from the Protein Data Bank (PDB).[37] As shown in Figure 2, the active site is intact/closed in this structure and contains the expected three Mg^{2+} ions, NSE triad, and DDXXD motif.[17] Lastly, a nucleophilic water molecule was present near Asn305 and Trp58. Chemically meaningful constraints were implemented throughout docking, i.e., the *TerDockin* approach was used.[36] Constraints are described below and in the SI. At least 2500 simulations were run per intermediate to reduce the impact of false positives and provide statistically meaningful information about orientations and interactions.[20,64] A filtration process was applied to remove docked poses that violated the constraints and to select the simulations with the best protein energy and interface energy scores (see SI for details).[36] This filtration process was also utilized when comparing docking modes to learn about enzymatic preferences. Lastly, Root Mean Square Deviation (RMSD) plots of intermediates were generated.[36]

In addition to performing docking on 1,8-cineole synthase in *Streptomyces clavuligerus*, the docking procedure was repeated for 1,8-cineole synthase in *Salvia fruticosa* (2J5C). Initial analysis of the crystal structure showed major drawbacks that would make the model a poor input for the *Terdockin* methodology, e.g., an incomplete DTE triad, missing Mg^{2+} ions, and water molecules in the active site associated with an open rather than closed conformation. Rather than using the crystal structure, we reconstructed the structure using AlphaFold and CHAI-1.[65–67] Models generated with

View Article Online
DOI: 10.1039/D6SC03024F

these methods were compared to terpene synthase crystal structures, such as that of (+)-bornyl diphosphate synthase, as an additional check of chemical and biological reasonability. The use of generative protein models can provide insight into the mechanistic details of terpene synthases, but we caution against making strong conclusions. Conformational searching was done for intermediates and transition structures using CREST (Conformer-Rotamer Ensemble Sampling Tool),[63] and small libraries of structures were generated for docking. The structures from CREST were filtered via QM optimization to remove duplicates. These libraries consisted of the lowest energy optimized structure from QM calculations and all structures within 5 kcal/mol.

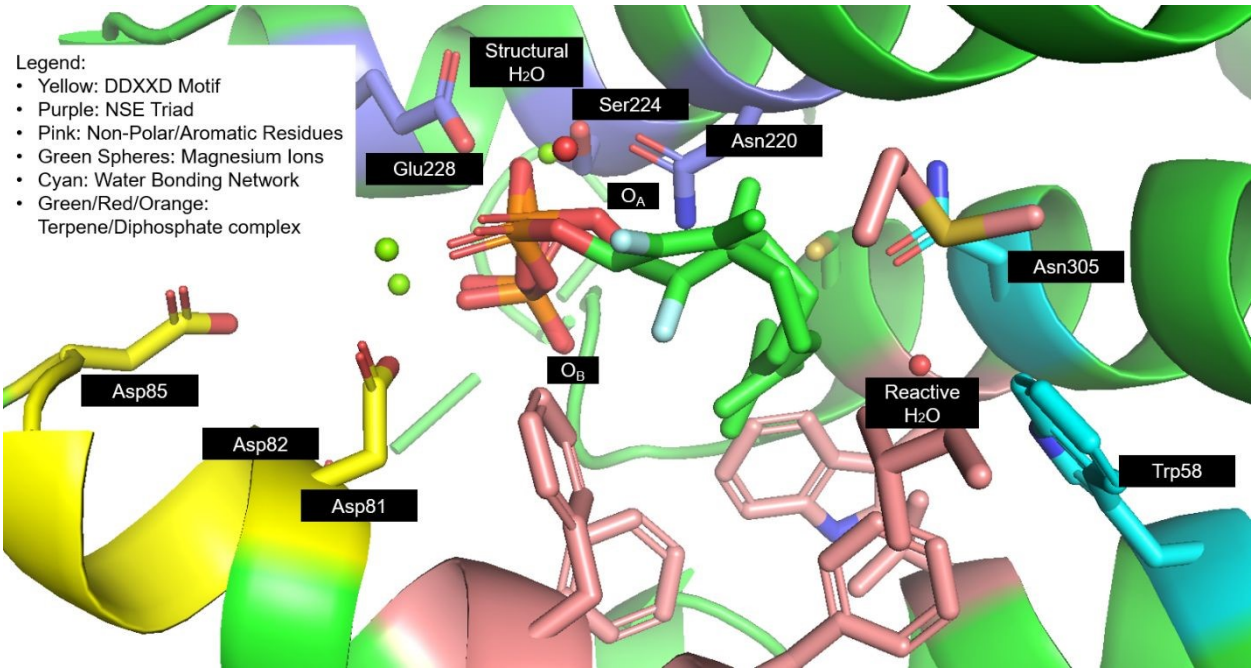

Figure 2. Active site of 1,8-cineole synthase in *Streptomyces clavuligerus* (5NX7).

Results and Discussion

View Article Online
DOI: 10.1039/D6SC03024F

DFT Studies

The proposed mechanism from Scheme 1 was predicted with DFT to have only low barriers, as shown in Figure 3. This result indicates that the carbocation, once generated, is inherently reactive enough to proceed rapidly to the product even without enzymatic intervention (at least if provided protective surroundings).[41] The σ-bond rotation step (via **TSAB**) was accompanied by a drop in free energy of approximately 10 kcal/mol, which is relatively large compared to the other steps in this mechanism. This step is so exergonic because an OH•••π interaction is formed.[68–70] In **B**, there is a strong interaction between the filled carbon-carbon π orbital and the unfilled oxygen-hydrogen σ* antibonding orbital in the product, as shown in Figure 4. In addition, the partially positively charged hydrogen atom on the oxonium ion is attracted electrostatically to the electron-rich carbon-carbon π-bond. The next relatively large change in free energy occurs upon bicyclic ether formation. In this step, a tertiary carbocation is traded for a strong carbon-oxygen σ-bond and an oxonium ion.

View Article Online
DOI: 10.1039/D6SC03024F

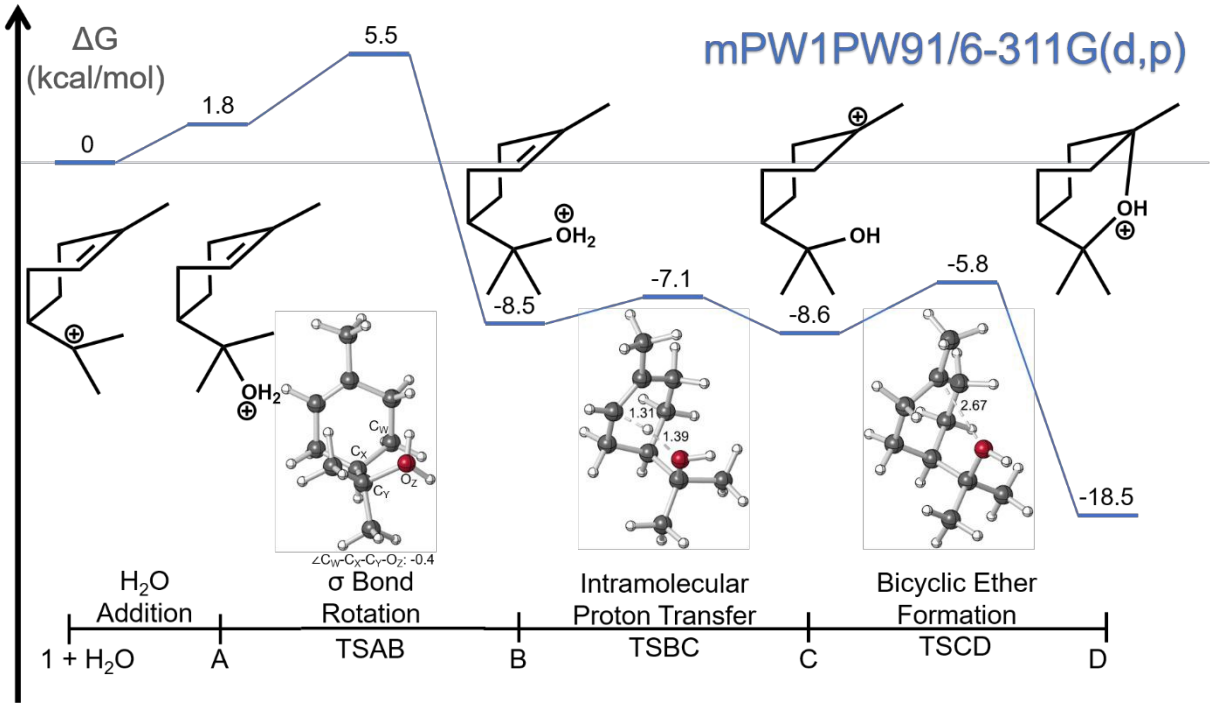

Figure 3. Reaction coordinate diagram from terpinyl cation to protonated 1,8-cineole at the mPW1PW91/6-311G(d,p) level of theory.

View Article Online
DOI: 10.1039/D6SC03024F

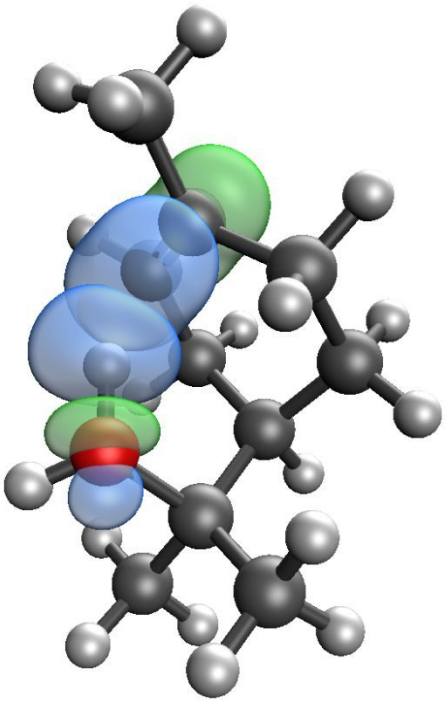

Figure 4. $\pi_{C\text{-}C} \leftrightarrow \sigma^*_{H\text{-}O}$ interaction which is 29.04 kcal/mol based on Second-Order Perturbation Theory.

Docking with 1,8-Cineole Synthase from *Streptomyces clavuligerus*

Before the intermediates from Scheme 1 were docked, a farnesyl pyrophosphate (FPP) analog, (*E*)-1-chloro-3,7-dimethylocta-2,6-diene, and its extensive conformer library were docked to help answer initial questions about active site orientation. The diphosphate group was replaced with a chlorine atom to speed up conformational searching and docking and to avoid artifacts associated with non-biological phosphate–substrate interactions.[36] Since the formation of 1,8-cineole involves initial conversion of geranyl diphosphate (**E**) to linalyl diphosphate intermediate (**G**/**H**) (Scheme 2),[72] there are four possible ways that the carbon backbone of the reacting carbocation could have been

View Article Online
DOI: 10.1039/D6SC03024F

bound to the diphosphate group; i.e., O_A and/or O_B of the diphosphate was at some point connected to C_A and C_B. Knowing the enzymatic preference between the four possibilities is important for subsequent docking experiments as it provides two necessary constraints between the diphosphate and the carbon backbone. These potential binding modes were tested via docking using distance constraints between the OPP and (*E*)-1-chloro-3,7-dimethylocta-2,6-diene, and only two out of the four passed the filtering (Table 1). O_B was thereby eliminated as the oxygen bound in **E.** Consequently, subsequent work involved only constraints from C_A to O_A and from C_B to either O_A or O_B.

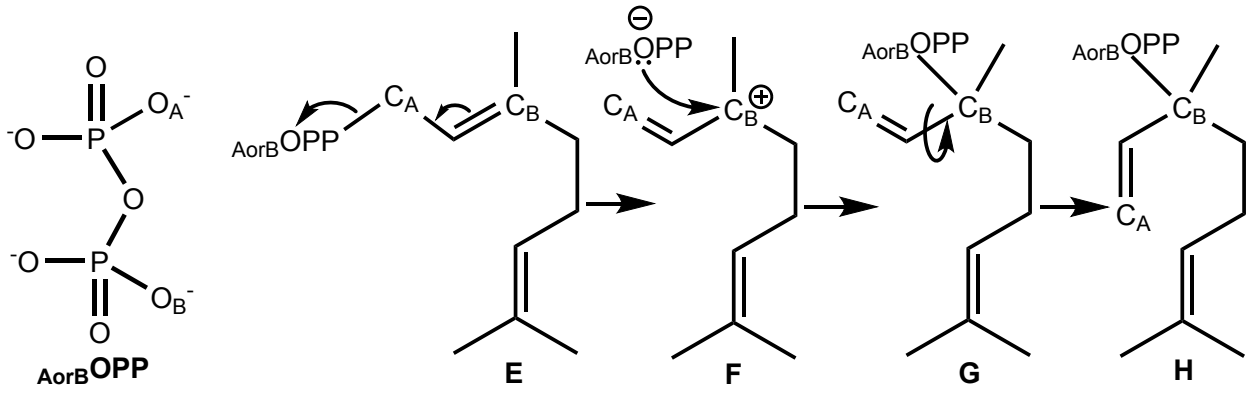

Scheme 2. Isomerization of geranyl diphosphate.

	$O_A \rightarrow O_A$	$O_A \rightarrow O_B$	$O_B \rightarrow O_A$	$O_B \rightarrow O_B$
$C_A \rightarrow C_B$	50	11	0	0

Table 1. Number of successful docking simulations for the four diphosphate-carbon docking modes.

View Article Online
DOI: 10.1039/D6SC03024F

Is There a Preference for One Enantiomer and/or One Conformer of the Terpinyl Cation?

Potential terpinyl cation intermediates (*R*)-**1** and (*S*)-**1** (Scheme 1) were docked into the 1,8-cineole synthase active site. For these intermediates, conformer libraries were split into two groups: those with axial and those with equatorial $C^+(CH_3)_2$ groups. A previous study suggested that having this group equatorial tends to lead to the production of monocyclic products, while having it axial leads to bicyclic product formation.[72] Thus, a conformational preference here could provide insight into the selectivity for 1,8-cineole over α-terpineol. Pooling and filtering the results of 5000 docking simulations each for the four docking modes revealed an overwhelming preference for $O_A \rightarrow O_A$ binding modes over $O_A \rightarrow O_B$ binding modes (Table 2), suggesting strongly O_A is the atom that reattaches to **F** (Scheme 2). No significant preference for the *R* or *S* form of the carbocation was found, however. This is perhaps not surprising given the very small difference in these structures – an interchange of only CH_2 and CH groups. Below, we address whether other enantiomeric carbocations can be differentiated.

	***R* Pathway**		***S* Pathway**	
Docking Mode	**$O_A \rightarrow O_A$**	**$O_A \rightarrow O_B$**	**$O_A \rightarrow O_A$**	**$O_A \rightarrow O_B$**
1_Axial	98	0	90	0
1_Equatorial	123	0	93	0

Table 2. Number of successful docking simulations when comparing $O_A \rightarrow O_A$ docking modes to $O_A \rightarrow O_B$ docking modes.

What is the Base that Deprotonates Intermediate **D**?

View Article Online
DOI: 10.1039/D6SC03024F

Previous computational work showed that Asn305 is a viable base for deprotonating oxonium ion **D** (Scheme 1).[40] However, there are other potential basic groups in the active site: two diphosphate oxygen atoms (O_A and O_B) and an alternative asparagine (Asn220) (Figure 2). Both diphosphate groups and asparagine residues acting as bases have precedent.[73,74] While Asn305 hydrogen bonds with a water molecule, Asn220 is part of the NSE triad commonly seen in Class I terpene synthases.[17] Table 3 shows the number of successful docking simulations for each possible base, using both enantiomers of oxonium ion **D** (note that here, the difference in enantiomers is a result of the direction the O–H bond points). Based on these results, only O_B (for both *R* and *S*) and Asn305 (only for *R*) can be confidently ruled out. RMSD analysis comparing non-hydrogen atoms between docked cations **C** and **D** (Scheme 1 and Figure 5)[20,64] indicates preferences among the remaining candidates, however. For the *R* pathway, O_A as the base is preferred, while for the *S* pathway, Asn305 is preferred, although not as strongly. Given that results from Dickschat's previous labeling experiments indicate that the *S* pathway is followed,[49] it appears that the previous assumption that Asn305 acts as a base is entirely reasonable.[37,40] However, we point out that both O_A and Asn220 also appear to be viable. The presence of multiple viable bases may enhance the preference for the *S* pathway.

Potential Base	*R* Pathway	*S* Pathway
O_A	31	37
O_B	0	2
Asn220	20	37
Asn305	1	37

Table 3. Number of successful simulations for Intermediate D.

View Article Online
DOI: 10.1039/D6SC03024F

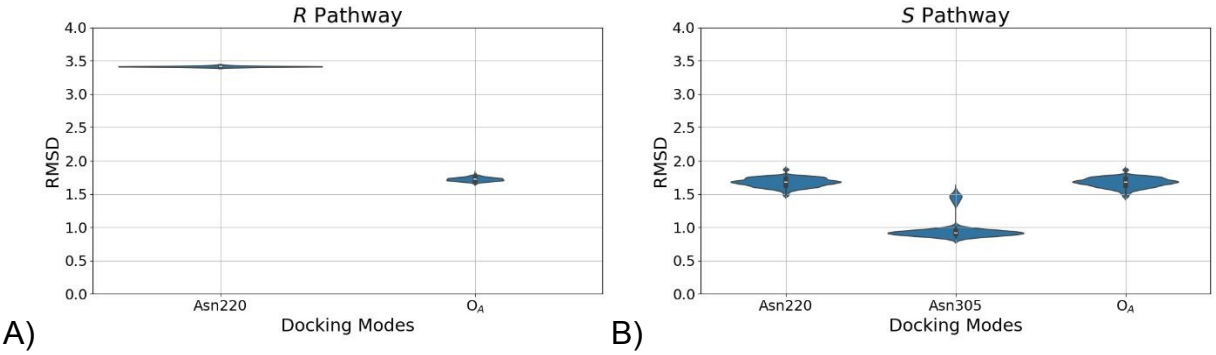

A) B)

Figure 5. RMSD analysis for **C** and **D**. The x-axis label is the conditional base. A) The *R* pathway. B) The *S* pathway.

Are *S* Enantiomers of Other Intermediates Preferred?

Table 4 shows the number of successful docking simulations for enantiomers of all cationic intermediates. Cations **B**, **C**, and **D** (Scheme 1) all have preferences for the *S* pathway, although that for **C** is not large. While both *R* and *S* versions of **1** and **A** have viable pathways, an equatorial cationic group is preferred for *R* and an axial cationic group is preferred for *S*. As mentioned above, an axial preference is associated with less side product formation (bicyclic products) and the bacterial 1,8-cineole synthase we are examining here is reported to have minimal side product accumulation (see SI for modeling of side product formation).[37,40] In sum, this evidence is consistent with the *S* pathway predominating. However, although the *TerDockin* data is suggestive, it is not definitive.

View Article Online
DOI: 10.1039/D6SC03024F

***R* Isomer**			***S* Isomer**		
	$O_A \rightarrow O_A$			$O_A \rightarrow O_A$	
(R)-1	Axial: 35	Equatorial: 157	(S)-1	Axial: 87	Equatorial: 0
A	Axial: 2	Equatorial: 138	A	Axial: 129	Equatorial: 0
B	26		B	124	
C	59		C	96	
D	3		D	87	

Table 4. Number of successful docking simulations when comparing the *R* pathway to the *S* pathway.

Why do *R* and *S* pathways Involve Different Bases?

Figure 6 shows the predicted preferred binding modes for all intermediates in the *S* and *R* pathways. In the *S* pathway, the oxygen atom is predicted to rotate towards Asn220 and Asn305 (towards the back as depicted), whereas the opposite is seen for the *R* pathway. These movements point the oxonium ion towards the two asparagine residues in the *S* pathway.

View Article Online
DOI: 10.1039/D6SC03024F

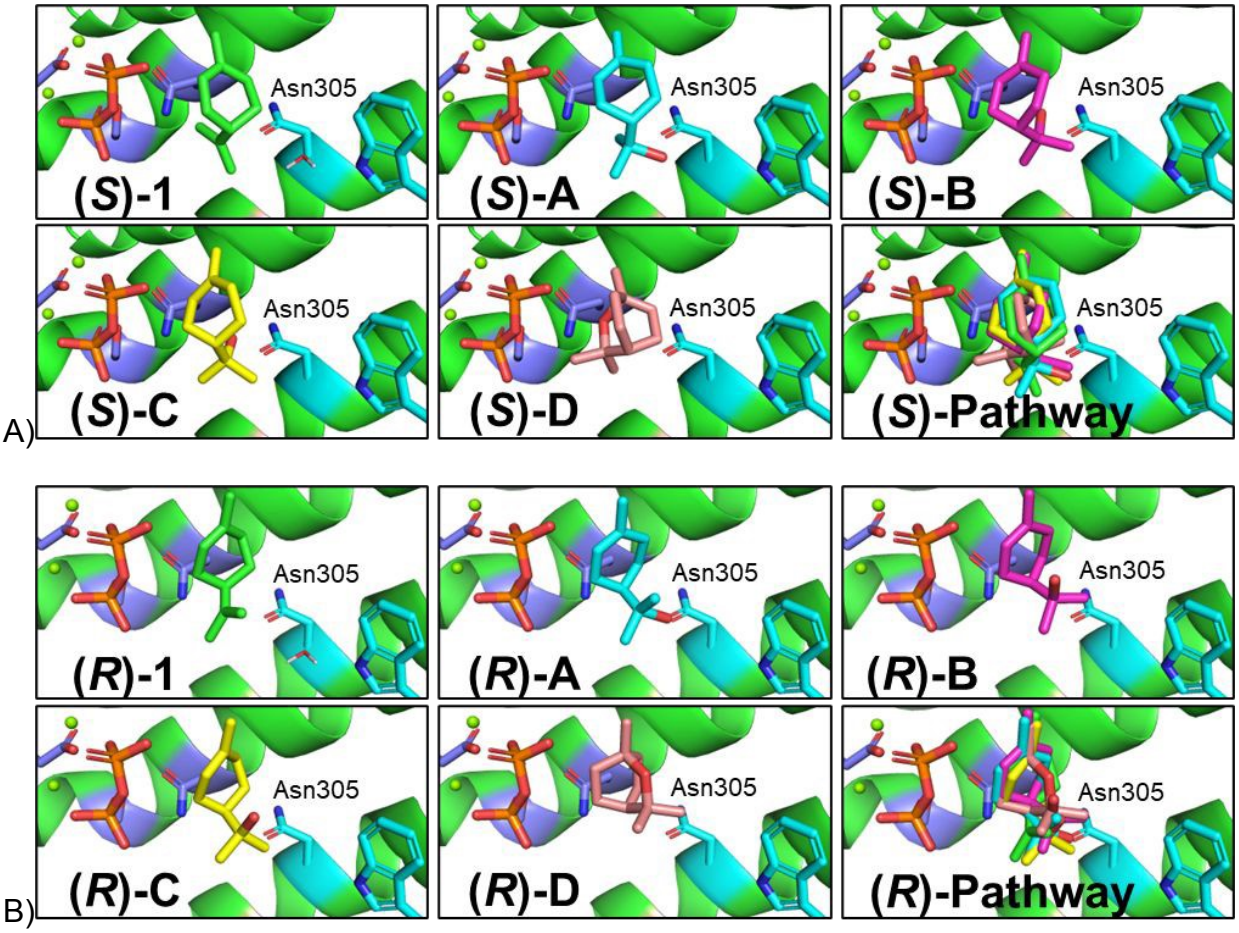

Figure 6. Docking poses for the A) *S* and B) *R* pathways. Final images show all structures superimposed. Light blue depicts Asn305 while dark blue depicts Asn220. See Figure S3 for RMSD analyses.

Docking with 1,8-Cineole Synthase from *Salvia fruticosa*

AlphaFold and CHAI-1 generated five models each, and from the predicted Local Distance Difference Test (plDDT),[75] the bulk of the enzyme (including most of the active site) was in the confident or greater region. The N-terminus, however, was in the low-confidence region, which raises concern, as the N-terminus often acts as a lid once the

View Article Online
DOI: 10.1039/D6SC03024F

substrate enters the active site.[21] This inaccuracy was more prevalent in the AlphaFold models compared to the CHAI-1 models (Figure 7a). In addition, CHAI-1 was able to include both geranyl diphosphate and Mg^{2+} ions, whereas AlphaFold was only able to include Mg^{2+} ions. Moving forward, only the results obtained with CHAI-1 models were considered. The best CHAI-1 model was compared to the X-ray structures of 1,8-cineole synthase from *Salvia fruticosa* (2J5C) (α-carbon RMSD of 0.68 Å) and (+)-bornyl diphosphate synthase from *Salvia officinalis* (1N23) (α-carbon RMSD of 0.99 Å). The catalytic Asn338 and Trp317 were present, along with reasonable space to accommodate water molecules (Figure 7b). On the diphosphate side, the DDXXD motif and DTE triad interacted with the Mg^{2+} and diphosphate moieties as expected. Overall, while generative models are not perfect, the CHAI-1 model appeared reasonable enough to pursue docking.

View Article Online
DOI: 10.1039/D6SC03024F

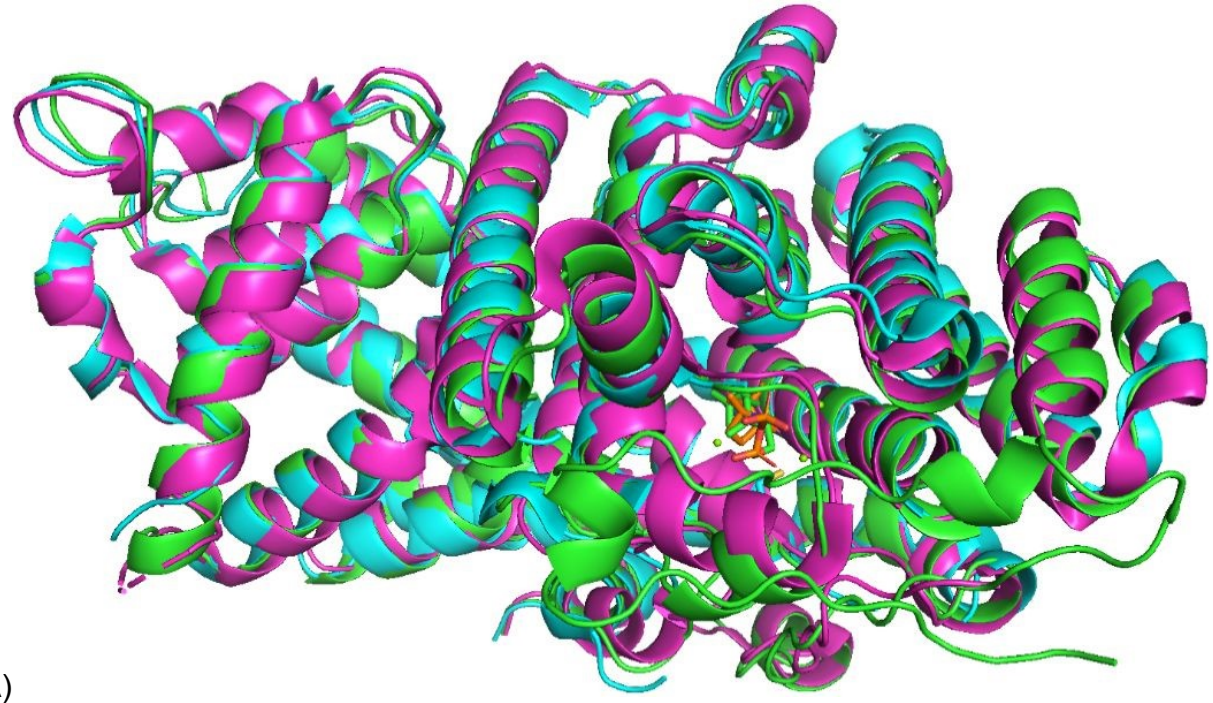

A)

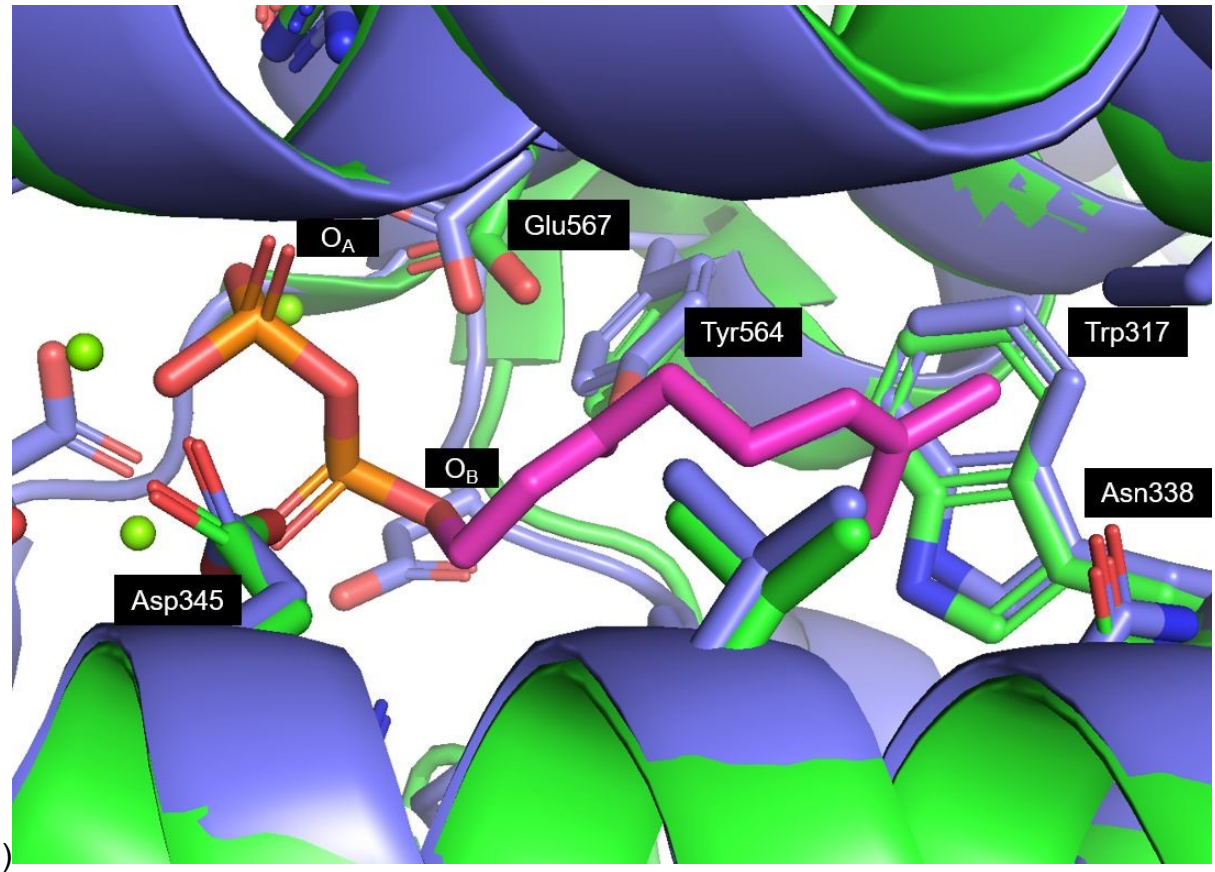

B)

View Article Online
DOI: 10.1039/D6SC03024F

Figure 7. A) Overlay of CHAI-1 generated model (green), crystal structure of 2J5C (cyan), and crystal structure of 1N23 (pink). B) Overlay of the active site of the CHAI-1 generated model and 2J5C crystal structure.

TerDockin results (Table 5) show a strong preference for O_B of the diphosphate to be connected to C_A of (*E*)-1-chloro-3,7-dimethylocta-2,6-diene across all criteria, including a new criterion of distance to the reactive water molecule. When docking (*R*)-**1** and (*S*)-**1** (Scheme 1) in the active site, a strong preference for O_B binding to C_B was also observed. This terpene-diphosphate binding prediction is opposite to the terpene-diphosphate preference seen in *Streptomyces clavuligerus* docking, likely due to subtle differences in relative positions of the diphosphate binding region and the Asn/Trp region in *Salvia fruticosa* and *Streptomyces clavuligerus* (compare Figures 2 and 7B). This difference in diphosphate-carbon binding orientation between plant and non-plant terpene cyclases was noted previously based on docking for cineole synthases.[76] Initial docking of (*R*)-**1** and (*S*)-**1** showed a large distance between the tertiary carbocation and the reactive water molecule (Figure 8A). The average distances between the axial (*R*)-**1** and (*S*)-**1** carbocations and the water molecule were 5.4 Å and 6.0 Å, respectively. Consequently, we hypothesized that a second water molecule might be present. Subsequent docking simulations included two water molecules near Asn338 and Trp317, and a reasonable hydrogen bonding network was established (Figure 8A). Both water molecules are coordinated with Asn338 and each other, while the structural water coordinates to Trp317. The distance between the new reactive water molecule and (*R*)

View Article Online
DOI: 10.1039/D6SC03024F

and (*S*)-**1** was reduced to 3.2 Å and 3.5 Å, respectively. Subsequent docking calculations included both water molecules.

	O_A - C_A	O_B - C_A
Number Passed	20	73
Total Score (REU)	-1800.5	-1820.3
Interface Energy (REU)	-9.5	-13.7
Distance to Catalytic Water (Å)	5.5	4.6

Table 5: Docking simulation data of (*E*)-1-chloro-3,7-dimethylocta-2,6-diene across with water and diphosphate present.

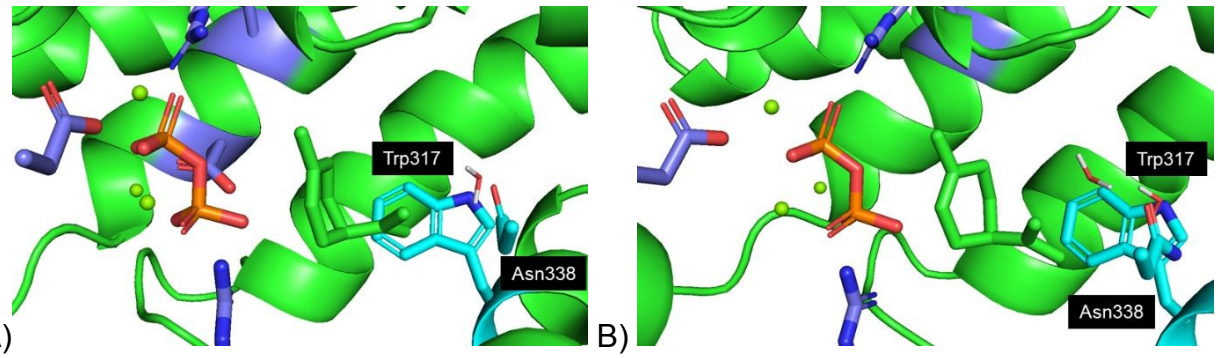

Figure 8. (*R*)-**1** docking modes with one (A) or two (B) water molecules. In cyan are Asn338 and Trp317, and in dark blue are various amino acids coordinating to the diphosphate/Mg^{2+} complex.

All intermediates present in Scheme 1 fit in the active site with many successful poses for both *R* and *S* pathways, as seen in Table 6. Tentatively, we ascribe the high

View Article Online
DOI: 10.1039/D6SC03024F

number of side products in *Salvia fruticosa* to the terpinyl cation having prevalent binding orientations in an equatorial conformation and the need for a second water molecule.

***R* Isomer**				***S* Isomer**			
	Number Passed	**Total Score**	**Interface Energy**		**Number Passed**	**Total Score**	**Interface Energy**
(R)-1	Axial: 113	-1846.5	-13.3	(S)-1	Axial: 109	-1841.8	-12.3
	Equatorial: 119	-1843.2	-13.1		Equatorial: 110	-1838.4	-13.3
A	Axial: 111	-1831.9	-11.7	A	Axial: 118	-1825.1	-11.7
	Equatorial: 73	-1818.8	-11.4		Equatorial: 116	-1824.5	-12.7
B	81	-1830.7	-12.4	B	84	-1831.9	-13.1
C	100	-1823.6	-12.3	C	107	-1827.5	-11.5
D	87	-1832.5	-13.3	D	86	-1831.9	-13.3

Table 6. Number of successful docking simulations of both *R* and *S* pathways in *Salvia fruticosa* (computed separately). The total score and interface energy are in Rosetta Energy Units (REU).

When the *R* and *S* pathway results are combined, a stereochemical preference was observed based on the number of passing poses, even though total score and interface energy values are similar (see Table 6). RMSD analysis indicates a relatively continuous pathway from the terpinyl cation to 1,8-cineole across both stereochemical pathways (see SI for RMSD plots), but deviations are higher compared to the values for 1,8-cineole synthase from *Streptomyces clavuligerus,* consistent with the observation of higher side product formation in *Salvia fruticosa*.

View Article Online
DOI: 10.1039/D6SC03024F

R Isomer		*S* Isomer	
	Number Passed		**Number Passed**
(R)-1	Axial: 224	(S)-1	Axial: 2
	Equatorial: 68		Equatorial: 162
A	Axial: 180	A	Axial: 44
	Equatorial: 2		Equatorial: 188
B	4	B	160
C	144	C	63
D	93	D	81

Table 7. Number of successful docking simulations when comparing the *R* pathway to the *S* pathway for 1,8-cineole synthase in *Salvia fruticosa* (pooled results).

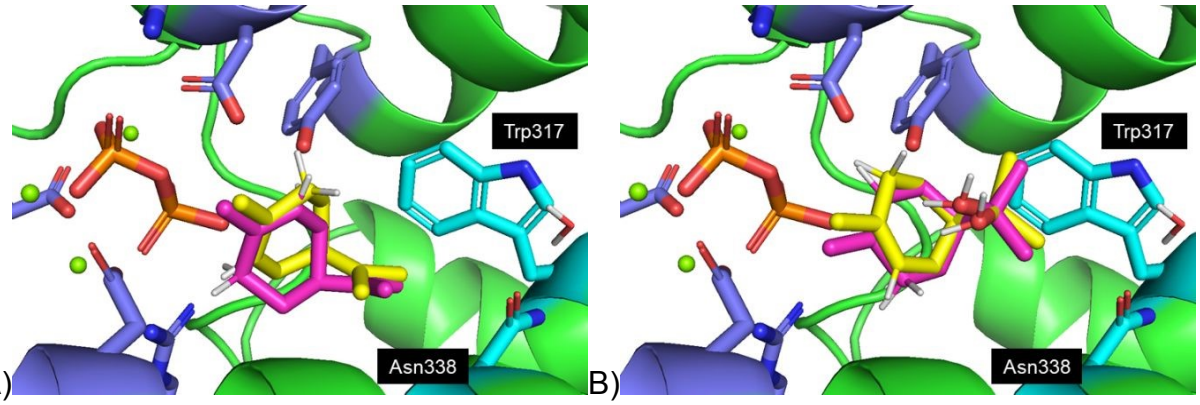

Figure 9. Overlay of Intermediates **1** and **B** for both *R* and *S* pathways. A) Intermediate **1,** where yellow is (*R*)-**1** and pink is (*S*)-**1**. B) Intermediate **B,** where yellow is (*R*)-**B** and pink is (*S*)-**B**.

View Article Online
DOI: 10.1039/D6SC03024F

Conclusions

The introduction of a water molecule by a terpene synthase creates a scenario where carbocation and oxonium ion reactivity must be balanced. In some cases, this balance is tipped toward ether formation. Here, we model one such case – 1,8-cineole formation – via the *TerDockin* approach. Our simulations not only show that *TerDockin* can capture this type of reactivity, but the results of this semi-automated/chemically informed docking approach led us to concrete, detailed models for 1,8-cineole formation. Based on our results, we agree with previous studies that Asn305 in *Streptomyces clavuligerus* 1,8-cineole synthase is a competent final base,[37,40] but we propose that Asn220 and one oxygen atom of bound diphosphate are also capable of playing this role. Our *TerDockin* simulations also suggest that the *S* pathway (Scheme 1) is preferred (although not strongly for all intermediates), which matches with the results of previous isotopic labeling experiments[49] (and conflicts with previous conclusions derived from analysis of the X-ray structure).[37] Our *TerDockin* results also indicate that the preferred *S* pathway involves conformations previously suggested to lead to fewer side products, consistent with the dearth of such products. In contrast, the absence of strong stereochemical and conformational preferences predicted for 1,8-cineole synthase from *Salvia fruticosa* is consistent with increased formation of side products in this organism.

Author Contributions

A. P.: Investigation, methodology, draft writing, lead data analysis, and lead figure making. J. B. S.: Guidance on TerDockin methodology, and final draft review. D. J. T.:

View Article Online
DOI: 10.1039/D6SC03024F

Supervision, funding acquisition, guidance on quantum mechanics and TerDockin modeling, and editing and review.

Conflict of Interest

There are no conflicts to declare.

Acknowledgements

We gratefully acknowledge financial support from the National Institutes of Health (1R35GM153469) and computational support from the National Science Foundation's ACCESS program (CHE240194). We are exceedingly grateful to Prof. Reuben Peters (Iowa State) for inspiring this project. We are appreciative of Ian Torrence's mentorship and guidance relating to all aspects of *TerDockin*.

Supporting Information

Data from DFT calculations, information on docking constraints, docking results data, and supplementary analysis.

View Article Online
DOI: 10.1039/D6SC03024F

References

(1) D. Tholl, in *Biotechnology of Isoprenoids*, ed. J. Schrader and J. Bohlmann, Springer International Publishing, Cham, 2015, pp. 63–106.
(2) D. J. McGarvey and R. Croteau, *Plant Cell*, 1995, **7**, 1015–1026, DOI: 10.1105/tpc.7.7.1015.
(3) F. Zhou and E. Pichersky, *Curr. Opin. Plant Biol.*, 2020, **55**, 1–10, DOI: 10.1016/j.pbi.2020.01.005.
(4) D. A. T. Boncan, S. S. K. Tsang, C. Li, I. H. T. Lee, H.-M. Lam, T.-F. Chan and J. H. L. Hui, *Int. J. Mol. Sci.*, 2020, **21**, 7382, DOI: 10.3390/ijms21197382.
(5) S. C. Roberts, *Nat. Chem. Biol.*, 2007, **3**, 387–395, DOI: 10.1038/nchembio.2007.8.
(6) A. C. Huang and A. Osbourn, *Pest Manag. Sci.*, 2019, **75**, 2368–2377, DOI: 10.1002/ps.5410.
(7) M. L. Del Prado-Audelo, H. Cortés, I. H. Caballero-Florán, M. González-Torres, L. Escutia-Guadarrama, S. A. Bernal-Chávez, D. M. Giraldo-Gomez, J. J. Magaña and G. Leyva-Gómez, *Front. Pharmacol.*, 2021, **12**, 704197, DOI: 10.3389/fphar.2021.704197.
(8) D. L. Klayman, *Science*, 1985, **228**, 1049–1055, DOI: 10.1126/science.3887571.
(9) M. C. Wani, H. L. Taylor, M. E. Wall, P. Coggon and A. T. McPhail, *J. Am. Chem. Soc.*, 1971, **93**, 2325–2327, DOI: 10.1021/ja00738a045.
(10) A. Masyita, R. M. Sari, A. D. Astuti, B. Yasir, N. R. Rumata, T. B. Emran, F. Nainu and J. Simal-Gandara, *Food Chem. X*, 2022, **13**, 100217, DOI: 10.1016/j.fochx.2022.100217.
(11) J. B. Sharmeen, F. M. Mahomoodally, G. Zengin and F. Maggi, *Molecules*, 2021, **26**, 666, DOI: 10.3390/molecules26030666.
(12) S. Sommer, L. M. Lang, L. Drummond, M. Buchhaupt, M. A. Fraatz and H. Zorn, *Molecules*, 2022, **27**, 3827, DOI: 10.3390/molecules27123827.
(13) L. Caputi and E. Aprea, *Recent Pat. Food Nutr. Agric.*, 2011, **3**, 9–16, DOI: 10.2174/2212798411103010009.
(14) R. Mewalal, D. K. Rai, D. Kainer, F. Chen, C. Külheim, G. F. Peter and G. A. Tuskan, *Trends Biotechnol.*, 2017, **35**, 227–240, DOI: 10.1016/j.tibtech.2016.08.003.
(15) J. S. Dambolena, M. P. Zunino, J. M. Herrera, R. P. Pizzolitto, V. A. Areco and J. A. Zygadlo, *Psyche J. Entomol.*, 2016, **2016**, 4595823, DOI: 10.1155/2016/4595823.
(16) J. A. Aaron and D. W. Christianson, *Pure Appl. Chem.*, 2010, **82**, 1585–1597, DOI: 10.1351/PAC-CON-09-09-37.
(17) D. W. Christianson, *Chem. Rev.*, 2017, **117**, 11570–11648, DOI: 10.1021/acs.chemrev.7b00287.
(18) X. Pan, J. D. Rudolf and L.-B. Dong, *Nat. Prod. Rep.*, 2024, **41**, 402–433, DOI: 10.1039/D3NP00033H.
(19) Y. J. Hong and D. J. Tantillo, *Org. Biomol. Chem.*, 2010, **8**, 4589–4600, DOI: 10.1039/C0OB00167H.
(20) T. E. O'Brien, S. J. Bertolani, Y. Zhang, J. B. Siegel and D. J. Tantillo, *ACS Catal.*, 2018, **8**, 3322–3330, DOI: 10.1021/acscatal.8b00342.
(21) D. A. Whittington, M. L. Wise, M. Urbansky, R. M. Coates, R. B. Croteau and D. W. Christianson, *Proc. Natl. Acad. Sci. U. S. A.*, 2002, **99**, 15375–15380, DOI: 10.1073/pnas.232591099.
(22) D. E. Cane, A. Saito, R. Croteau, J. Shaskus and M. Felton, *J. Am. Chem. Soc.*, 1982, **104**, 5831–5833, DOI: 10.1021/ja00385a067.
(23) M. Weitman and D. T. Major, *J. Am. Chem. Soc.*, 2010, **132**, 6349–6360, DOI: 10.1021/ja910134x.
(24) D. T. Major and M. Weitman, *J. Am. Chem. Soc.*, 2012, **134**, 19454–19462, DOI: 10.1021/ja308295p.
(25) B. Piechulla, R. Bartelt, A. Brosemann, U. Effmert, H. Bouwmeester, F. Hippauf and W. Brandt, *Plant Physiol.*, 2016, **172**, 2120–2131, DOI: 10.1104/pp.16.01378.
(26) J. Liang, J. Liu, R. Brown, M. Jia, K. Zhou, R. J. Peters and Q. Wang, *Plant J.*, 2018, **94**, 847–856, DOI: 10.1111/tpj.13901.

View Article Online
DOI: 10.1039/D6SC03024F

(27) E. M. Davis and R. Croteau, in *Biosynthesis: Aromatic Polyketides, Isoprenoids, Alkaloids*, ed. F. J. Leeper and J. C. Vederas, Springer, Berlin, Heidelberg, 2000, pp. 53–95, DOI: 10.1007/3-540-48146-X_2.
(28) Y. J. Hong and D. J. Tantillo, *J. Am. Chem. Soc.*, 2010, **132**, 5375–5386, DOI: 10.1021/ja9084786.
(29) G. B. Tabekoueng, B. Goldfuss and J. S. Dickschat, *Org. Lett.*, 2025, **27**, 10821–10824, DOI: 10.1021/acs.orglett.5c03451.
(30) Z.-Y. Huang, K. Xu, W.-L. Li, C.-X. Li, J. Pan, R. Wu and J.-H. Xu, *J. Am. Chem. Soc.*, 2025, **147**, 45822–45831, DOI: 10.1021/jacs.5c19381.
(31) M. N. Gaynes, K. R. Osika and D. W. Christianson, *Biochemistry*, 2025, **64**, 4830–4840, DOI: 10.1021/acs.biochem.5c00565.
(32) S. Mafu, K. C. Potter, M. L. Hillwig, S. Schulte, J. Criswell and R. J. Peters, *Chem. Commun.*, 2015, **51**, 13485–13487, DOI: 10.1039/C5CC05754J.
(33) I. Pateraki, J. Andersen-Ranberg, B. Hamberger, A. M. Heskes, H. J. Martens, P. Zerbe, S. S. Bach, B. L. Møller, J. Bohlmann and B. Hamberger, *Plant Physiol.*, 2014, **164**, 1222–1236, DOI: 10.1104/pp.113.228429.
(34) M. L. Wise, M. Urbansky, G. L. Helms, R. M. Coates and R. Croteau, *J. Am. Chem. Soc.*, 2002, **124**, 8546–8547, DOI: 10.1021/ja0265714.
(35) L. Wang, J. Liang, X. Xie, J. Liu, Q. Shen, L. Li and Q. Wang, *Plant Mol. Biol.*, 2021, **105**, 55–64, DOI: 10.1007/s11103-020-01068-x.
(36) I. S. Torrence, T. E. O'Brien, J. B. Siegel and D. J. Tantillo, in *Methods in Enzymology*, ed. J. Rudolf, Academic Press, 2024, vol. 699, pp. 231–263, DOI: 10.1016/bs.mie.2024.02.006.
(37) V. Karuppiah, K. E. Ranaghan, N. G. H. Leferink, L. O. Johannissen, M. Shanmugam, A. Ní Cheallaigh, N. J. Bennett, L. J. Kearsey, E. Takano, J. M. Gardiner, M. W. van der Kamp, S. Hay, A. J. Mulholland, D. Leys and N. S. Scrutton, *ACS Catal.*, 2017, **7**, 6268–6282, DOI: 10.1021/acscatal.7b01924.
(38) R. Croteau and F. Karp, *Arch. Biochem. Biophys.*, 1977, **179**, 257–265, DOI: 10.1016/0003-9861(77)90110-2.
(39) R. Croteau, W. R. Alonso, A. E. Koepp and M. A. Johnson, *Arch. Biochem. Biophys.*, 1994, **309**, 184–192, DOI: 10.1006/abbi.1994.1101.
(40) N. G. H. Leferink, K. E. Ranaghan, J. Battye, L. O. Johannissen, S. Hay, M. W. van der Kamp, A. J. Mulholland and N. S. Scrutton, *ChemBioChem*, 2020, **21**, 985–990, DOI: 10.1002/cbic.201900672.
(41) D. J. Tantillo, *Angew. Chem. Int. Ed Engl.*, 2017, **56**, 10040–10045, DOI: 10.1002/anie.201702363.
(42) N. G. H. Leferink, A. J. Jervis, Z. Zebec, H. S. Toogood, S. Hay, E. Takano and N. S. Scrutton, *ChemistrySelect*, 2016, **1**, 1893–1896, DOI: 10.1002/slct.201600563.
(43) C. Nakano, H.-K. Kim and Y. Ohnishi, *ChemBioChem*, 2011, **12**, 1988–1991, DOI: 10.1002/cbic.201100330.
(44) S. C. Kampranis, D. Ioannidis, A. Purvis, W. Mahrez, E. Ninga, N. A. Katerelos, S. Anssour, J. M. Dunwell, J. Degenhardt, A. M. Makris, P. W. Goodenough and C. B. Johnson, *Plant Cell*, 2007, **19**, 1994–2005, DOI: 10.1105/tpc.106.047779.
(45) N. Badalamenti, G. Salbitani, P. Cianciullo, R. Bossa, F. De Ruberto, V. Greco, A. Basile, V. Maresca, M. Bruno and S. Carfagna, *Antioxidants*, 2023, **12**, 1990, DOI: 10.3390/antiox12111990.
(46) K. Raz, S. Levi, P. K. Gupta and D. T. Major, *Curr. Opin. Biotechnol.*, 2020, **65**, 248–258, DOI: 10.1016/j.copbio.2020.06.002.
(47) D. T. Major, Y. Freud and M. Weitman, *Curr. Opin. Chem. Biol.*, 2014, **21**, 25–33, DOI: 10.1016/j.cbpa.2014.03.010.
(48) M. L. Wise, T. J. Savage, E. Katahira and R. Croteau, *J. Biol. Chem.*, 1998, **273**, 14891–14899, DOI: 10.1074/jbc.273.24.14891.
(49) J. Rinkel, P. Rabe, L. Zur Horst and J. S. Dickschat, *Beilstein J. Org. Chem.*, 2016, **12**, 2317–2324, DOI: 10.3762/bjoc.12.225.

View Article Online
DOI: 10.1039/D6SC03024F

(50) M. J. Frisch, G. W. Trucks, H. B. Schlegel, G. E. Scuseria, M. A. Robb, J. R. Cheeseman, G. Scalmani, V. Barone, G. A. Petersson, H. Nakatsuji, X. Li, M. Caricato, A. V. Marenich, J. Bloino, B. G. Janesko, R. Gomperts, B. Mennucci, H. P. Hratchian, J. V. Ortiz, A. F. Izmaylov, J. L. Sonnenberg, D. Williams-Young, F. Ding, F. Lipparini, F. Egidi, J. Goings, B. Peng, A. Petrone, T. Henderson, D. Ranasinghe, V. G. Zakrzewski, J. Gao, N. Rega, G. Zheng, W. Liang, M. Hada, M. Ehara, K. Toyota, R. Fukuda, J. Hasegawa, M. Ishida, T. Nakajima, Y. Honda, O. Kitao, H. Nakai, T. Vreven, K. Throssell, J. A. Montgomery, Jr., J. E. Peralta, F. Ogliaro, M. J. Bearpark, J. J. Heyd, E. N. Brothers, K. N. Kudin, V. N. Staroverov, T. A. Keith, R. Kobayashi, J. Normand, K. Raghavachari, A. P. Rendell, J. C. Burant, S. S. Iyengar, J. Tomasi, M. Cossi, J. M. Millam, M. Klene, C. Adamo, R. Cammi, J. W. Ochterski, R. L. Martin, K. Morokuma, O. Farkas, J. B. Foresman and D. J. Fox, Gaussian 16 (Revision C.01) Gaussian, Inc., Wallingford CT, 2016.

(51) A. D. Becke, *J. Chem. Phys.*, 1993, **98**, 1372–1377, DOI: 10.1063/1.464304.

(52) J. Tirado-Rives and W. L. Jorgensen, *J. Chem. Theory Comput.*, 2008, **4**, 297–306, DOI: 10.1021/ct700248k.

(53) D. J. Tantillo, *Nat. Prod. Rep.*, 2011, **28**, 1035–1053, DOI: 10.1039/C1NP00006C.

(54) S. P. T. Matsuda, W. K. Wilson and Q. Xiong, *Org. Biomol. Chem.*, 2006, **4**, 530–543, DOI: 10.1039/B513599K.

(55) R. Ditchfield, W. J. Hehre and J. A. Pople, *J. Chem. Phys.*, 1971, **54**, 724–728, DOI: 10.1063/1.1674902.

(56) G. Luchini, J. V. Alegre-Requena, I. Funes-Ardoiz and R. S. Paton, *F1000Research*, 2020, **9**, DOI: 10.12688/f1000research.22758.1.

(57) E. D. Glendening, C. R. Landis and F. Weinhold, *J. Comput. Chem.,* 2019, **40**, 2234–2241. DOI: 10.1002/jcc.25873

(58) F. Weinhold, C. R. Landis and E. D. Glendening, *Int. Rev. Phys. Chem.*, 2016, **35**, 399–440, DOI: 10.1080/0144235X.2016.1192262.

(59) E. D. Glendening, J. K. Badenhoop, A. E. Reed, J. E. Carpenter, J. A. Bohmann, C. M. Morales, P. Karafiloglou, C. R. Landis and F. Weinhold, *NBO 7.0*, Theoretical Chemistry Institute, University of Wisconsin, Madison, 2018.

(60) A. Leaver-Fay, M. Tyka, S. M. Lewis, O. F. Lange, J. Thompson, R. Jacak, K. Kaufman, P. D. Renfrew, C. A. Smith, W. Sheffler, I. W. Davis, S. Cooper, A. Treuille, D. J. Mandell, F. Richter, Y.-E. A. Ban, S. J. Fleishman, J. E. Corn, D. E. Kim, S. Lyskov, M. Berrondo, S. Mentzer, Z. Popović, J. J. Havranek, J. Karanicolas, R. Das, J. Meiler, T. Kortemme, J. J. Gray, B. Kuhlman, D. Baker and P. Bradley, *Methods Enzymol.*, 2011, **487**, 545–574, DOI: 10.1016/B978-0-12-381270-4.00019-6.

(61) J. Meiler and D. Baker, *Proteins*, 2006, **65**, 538–548, DOI: 10.1002/prot.21086.

(62) R.F. Alford, A. Leaver-Fay, J. R. Jeliazkov, M. J. O'Meara, F. P. DiMaio, H. Park, M. V. Shapovalov, P. D. Renfrew, V. K. Mulligan, K. Kappel, J. W. Labonte, M. S. Pacella, R. Bonneau, P. Bradley, R. L. Dunbrack Jr., R. Das, D. Baker, B. Kuhlman, T. Kortemme and J. J. Gray, *J. Chem. Theory Comput.*, 2017, **13**, 3031–3048, DOI: 10.1021/acs.jctc.7b00125.

(63) P. Pracht, F. Bohle and S. Grimme, *Phys. Chem. Chem. Phys.*, 2020, **22**, 7169–7192, DOI: 10.1039/C9CP06869D.

(64) T. E. O'Brien, S. J. Bertolani, D. J. Tantillo and J. B. Siegel, *Chem. Sci.*, 2016, **7**, 4009–4015, DOI: 10.1039/C6SC00635C.

(65) J. Abramson, J. Adler, J. Dunger, R. Evans, T. Green, A. Pritzel, O. Ronneberger, L. Willmore, A. J. Ballard, J. Bambrick, S. W. Bodenstein, D. A. Evans, C.-C. Hung, M. O'Neill, D. Reiman, K. Tunyasuvunakool, Z. Wu, A. Žemgulytė, E. Arvaniti, C. Beattie, O. Bertolli, A. Bridgland, A. Cherepanov, M. Congreve, A. I. Cowen-Rivers, A. Cowie, M. Figurnov, F. B. Fuchs, H. Gladman, R. Jain, Y. A. Khan, C. M. R Low, K. Perlin, A. Potapenko, P. Savy, S. Singh, A. Stecula, A. Thillaisundaram, C. Tong, S. Yakneen, E. D. Zhong, M. Zielinski, A. Žídek, V. Bapst, P. Kohli, M.

View Article Online
DOI: 10.1039/D6SC03024F

Jaderberg, D. Hassabis and J. M. Jumper, *Nature*, 2024, **630**, 493–500, DOI: 10.1038/s41586-024-07487-w.

(66) J. Jumper, R. Evans, A. Pritzel, T. Green, M. Figurnov, O. Ronneberger, K. Tunyasuvunakool, R. Bates, A. Žídek, A. Potapenko, A. Bridgland, C. Meyer, S. A. A. Kohl, A. J. Ballard, A. Cowie, B. Romera-Paredes, S. Nikolov, R. Jain, J. Adler, T. Back, S. Petersen, D. Reiman, E. Clancy, M. Zielinski, M. Steinegger, M. Pacholska, T. Berghammer, S. Bodenstein, D. Silver, O. Vinyals, A. W. Senior, K. Kavukcuoglu, P. Kohli and D. Hassabis, *Nature*, 2021, **596**, 583–589, DOI: 10.1038/s41586-021-03819-2.

(67) C. Discovery, J. Boitreaud, J. Dent, M. McPartlon, J. Meier, V. Reis, A. Rogozhnikov and K. Wu, *bioRxiv*, 2024, preprint, DOI: 10.1101/2024.10.10.615955.

(68) M. Durec, R. Marek and J. Kozelka, *Chem. – Eur. J.*, 2018, **24**, 5849–5859, DOI: 10.1002/chem.201705364.

(69) J. Novotný, S. Bazzi, R. Marek and J. Kozelka, *Phys. Chem. Chem. Phys.*, 2016, **18**, 19472–19481, DOI: 10.1039/C6CP01524G.

(70) T. van Mourik, S. L. Price and D. C. Clary, *Chem. Phys. Lett.*, 2000, **331**, 253–261, DOI: 10.1016/S0009-2614(00)01168-4.

(71) R. Croteau, J. Gershenzon, C. J. Wheeler and D. M. Satterwhite, *Arch. Biochem. Biophys.*, 1990, **277**, 374–381, DOI: 10.1016/0003-9861(90)90593-n.

(72) H. Kim, N. Srividya, I. Lange, E. W. Huchala, B. Ginovska, B. M. Lange and S. Raugei, *ACS Catal.*, 2022, **12**, 7453–7469, DOI: 10.1021/acscatal.2c01836.

(73) J. Xu, Y. Ai, J. Wang, J. Xu, Y. Zhang and D. Yang, *Phytochemistry*, 2017, **137**, 34–41, DOI: 10.1016/j.phytochem.2017.02.017.

(74) K. Zhou and R. J. Peters, *Chem. Commun. Camb. Engl.*, 2011, **47**, 4074–4080, DOI: 10.1039/c0cc02960b.

(75) V. Mariani, M. Biasini, A. Barbato and T. Schwede, *Bioinformatics*, 2013, **29**, 2722–2728, DOI: 10.1093/bioinformatics/btt473.

(76) R. Schwartz, S. Zev, and D. T. Major, *Angew. Chem. Int. Ed.*, 2024, **63**, e202400743.

View Article Online
DOI: 10.1039/D6SC03024F

- Data for this article, including computed coordinates are available at iochem-BD at https://doi.org/10.19061/iochem-bd-6-611.